Journal of Statistical Physics, Vol. 83, Nos. 1/2, 1996

Scars of Periodic Orbits in the Stadium Action Billiard

J. S. Espinoza Ortiz,[1] M. A. M. de Aguiar,[1] and A. M. Ozorio de Almeida[1]

Received September 20, 1994; final January 13, 1995

Compact billiards in phase space, or action billiards, are constructed by truncating the classical Hamiltonian in the action variables. The corresponding quantum mechanical system has a finite Hamiltonian matrix. In previous papers we defined the compact analog of common billiards, i.e., straight motion in phase space followed by specular reflections at the boundaries. Computation of their quantum energy spectra establishes that their properties are exactly those of common billiards: the short-range statistics follow the known universality classes depending on the regular or chaotic nature of the motion, while the long-range fluctuations are determined by the periodic orbits. In this work we show that the eigenfunctions also follow qualitatively the general characteristics of common billiards. In particular, we show that the low-lying levels can be classified according to their nodal lines as usual and that the high excited states present scars of several short periodic orbits. Moreover, since all the eigenstates of action billiards can be computed with great accuracy, Bogomolny's semiclassical formula for the scars can also be tested successfully.

KEY WORDS: Billiards; periodic orbits; scars; semiclassical limit.

1. INTRODUCTION

The concept of action billiards[3] realizes the practical need to truncate quantum mechanical Hamiltonian matrices when performing numerical diagonalizations. In the case where the matrices are written in terms of harmonic oscillator basis states, the truncation at a given quantum number N has a clear classical interpretation: it corresponds to a cutoff in the classical motion at the value $h(N+1/2)$ of the action variable. The idea of an action

[1] Instituto de Física "Gleb Wataghin," Universidade Estadual de Campinas, Campinas 13083-970, São Paulo, Brazil.

0022-4715/96/0400-0275$09.50/0

billiard is therefore to define a quantum mechanical system as a finite block of a given (infinite) Hamiltonian matrix, like the block one actually diagonalizes on a computer. The classical analog of such systems has its motion limited not in coordinate space, but in action space, hence their name *action billiards.*

In a previous paper[3] the classical cutoff in the action variables was studied in detail. We showed that the angle variables suffer a discontinuous jump when a trajectory hits the action boundary and the connection rule for the angles before and after the collision, was derived. In the extreme case of a harmonic oscillator, no trajectory ever hits the boundary and the truncation has no classical or quantum effect.[4] On the other hand, for Hamiltonians depending only on the angles, all trajectories will eventually hit the billiard boundary. These systems are the analog of common billiards, and it has been shown[1,2] that the statistical properties of their energy spectra follow exactly those of common billiards, i.e., the short-range statistics follow the known universality classes, whereas the long-range correlations are dictated by the periodic orbits.

From the point of view of semiclassical theory, the Hamiltonian to be considered in this paper [see Eq. (1)] is an extreme example of a non-kinetic-plus-potential system. Although the earlier derivations of the semiclassical limits only considered that kind of problem, more recent results based on phase space representations[8,9] have shown that the general theory works for any kind of Hamiltonian, including the type described here.

In this work we take a step forward in the study of these types of action billiards by analyzing in detail the wavefunctions in a stadium-shaped billiard. Our computations show that several individual eigenstates are scarred by the shortest periodic orbits of the stadium, much the same as for the wavefunctions of the common stadium billiard. Morever, since our diagonalization is exact, we are able to compute averages over several eigenstates of the probability density[5,6] providing another example of Bogomolny's theory of scars, which, as far as the authors know, has only once been previously tested.[7]

This paper is organized as follows: in Section 2 we define the stadium action billiard and review its most important properties. Section 3 presents the numerically computed wavefunctions, focusing on low-lying states and on scars of periodic orbits in highly excited states. We also apply Bogomolny's theory by averaging over groups of wavefunctions and show that, at places where the average energy corresponds to the quantized action of a classical orbit, its scar shows up very clearly in the averaged functions. Husimi distributions are also considered and some examples are given. Our conclusions are presented in Section 4.

2. THE STADIUM ACTION BILLIARD

The simplest two-dimensional Hamiltonian whose dynamics in the action variables space corresponds to motion along straight lines is given by[1]

$$H(I, \theta) = -\cos\theta_1 - \cos\theta_2 \tag{1}$$

where θ_i and I_i are action and angle variables for the harmonic oscillator $H_i = (p_i^2 + q_i^2)/2$. Indeed, since the action variables do not appear explicitly in H, Hamilton's equations can be integrated immediately, yielding

$$\begin{aligned} \theta_1(t) &= \theta_{10} = \text{const} \\ \theta_2(t) &= \theta_{20} = \text{const} \\ I_1(t) &= I_{10} - t\sin\theta_{10} \\ I_2(t) &= I_{20} - t\sin\theta_{20} \end{aligned} \tag{2}$$

which is analogous to a free particle in "coordinates" I and "momenta" θ. A classical action billiard is now constructed by limiting the accessible action space to a closed region. When a trajectory hits the boundary containing such a region, the "momenta" θ jump instantaneously. For the Hamiltonian above, it can be shown that the jump in the angles corresponds to a specular reflection at the boundary, exactly like the reflections in common billiards, as shown schematically in Fig. 1. Therefore, the shape of the billiard contour completely determines the nature of the classical motion.

The quantization of the Hamiltonian (1) can be achieved by writing

$$\cos\theta_i = \frac{q_i}{(q_i^2 + p_i^2)^{1/2}}$$

and using the usual step operators a and $a^\dagger$ for the harmonic oscillator H_i. Then

$$\hat{q}_i = \frac{\hat{a}_i + \hat{a}_i^\dagger}{\sqrt{2}}$$

$$\hat{p}_i^2 + \hat{q}_i^2 = \hat{a}_i^\dagger \hat{a}_i + \hat{a}_i \hat{a}_i^\dagger$$

and

$$\hat{H} = \frac{1}{\sqrt{2}} \sum_{i=1}^{2} \hat{a}_i \{\hat{a}_i^\dagger \hat{a}_i + \hat{a}_i \hat{a}_i^\dagger\}^{-1/2} + \{\hat{a}_i^\dagger \hat{a}_i + \hat{a}_i \hat{a}_i^\dagger\}^{-1/2} \hat{a}_i^\dagger \tag{3}$$

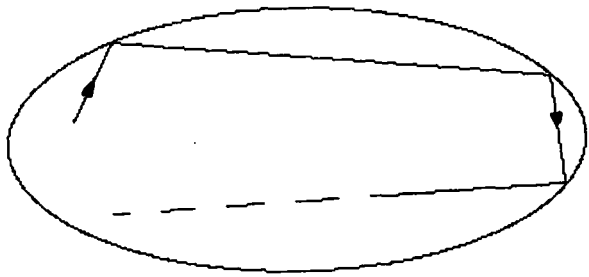

Fig. 1. Trajectory reflecting specularly at the bounderies of an action billiard.

where we have symmetrized the Hamiltonian to ensure the Hermitian property.

Once the classical boundary has been specified, the quantum mechanical billiard is obtained by computing the matrix elements

$$\langle n_1' n_2' |\, \hat{H}\, | n_1 n_2 \rangle = -\sum_{i=1}^{2} \frac{1}{\sqrt{2}} \left\{ \left(\frac{n_i}{n_i + \frac{1}{2}} \right)^{1/2} \delta_{n_i', n_{i-1}'} + \left(\frac{n_i + 1}{n_i + \frac{3}{2}} \right)^{1/2} \delta_{n_i', n_{i+1}'} \right\} \quad (4)$$

where the states $|nm\rangle$ are eigenstates of the two-dimensional harmonic oscillator $H_1 + H_2$ and the numbers (n_1, n_2) and (n_1', n_2') are such that their classical counterparts $I_i = (n_i + 1/2)\, h$ and $I_i' = (n_i' + 1/2)\, h$ lie inside the billiard contour. We shall call S this set of points. Although the quantum matrix is finite, its size increases as h^{-2} as $h \to 0$.

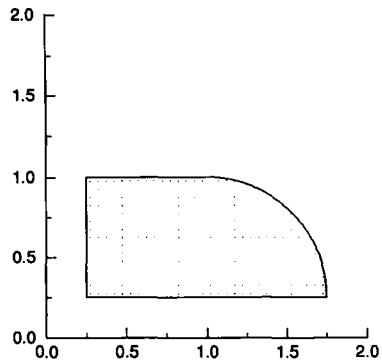

Fig. 2. Desymmetrized stadium billiard. The lattice points correspond to quantized actions $I_i = (n_i = 1/2)\, h$. In this example $h = 0.05$, which gives 404 lattice points, or basis states, inside the billiard contour.

In this paper we shall work with the desymmetrized stadium billliard, illustrated in Fig. 2, corresponding to the odd–odd eigenstates of the full stadium. The dimensions of the billiard are shown in the figure and they shall remain fixed throughout this work. The lattice points indicate the harmonic oscillator eigenstates from which the quantum matrix is built. In Fig. 2 the lattice illustrated corresponds to $h = 0.05$, but here we shall work with a smaller value, namely $h = 0.020$, which corresponds to a 2455×2455 quantum matrix. The position of the desymmetrized billiard in the (I_1, I_2) plane does not matter qualitatively if h is sufficiently small: any displacement of the billiard will not affect any of its quantum mechanical properties as long as its shape and area remain fixed.

As discussed in detail in ref. 1, the Weyl term of the average density of states can be calculated in closed form as

$$\eta_{\text{Weyl}}(E) = (8A/h^2\alpha_+)\, F(\alpha_-/\alpha_+) \tag{5}$$

where A is the billiard area in the action space,

$$\alpha_\pm = (1 \pm E/2)^2$$

and

$$F(k) = \int_0^{\pi/2} \frac{d\theta}{(1 - k^2 \sin^2\theta)^{1/2}}$$

is the complete elliptic integral of the first kind.

Defining a smoothed density of states as

$$\eta_\lambda(E) = \frac{1}{\lambda(2\pi)^{1/2}} \sum_n e^{-(E - E_n)^2/2\lambda^2}$$

where E_n are the eigenenergies, and subtracting from it the averaged Weyl term, we obtain the oscillatory function $\eta_{\text{osc}}(E)$, which can be studied via Fourier transforms. This study has been carried out in detail in ref. 1 where it has been shown that the maxima of the Fourier transform of $\eta_{\text{osc}}(E)$ correspond to periods of classical closed orbits. Here we shall be concerned mostly with the wavefunctions.

3. NUMERICAL RESULTS

In this section we present several numerical results concerning the eigenstates of the stadium action billiard. We show that the individual eigenstates exhibit scars of the shortest periodic orbits and that averaging the probability density over a group of neighboring states produces scars

in the way predicted by Bogomolny.[5] We also show projections of the Husimi distribution on the canonical planes (q_1, p_1) and (q_2, p_2) and compare them with the corresponding projections of periodic orbits. We emphasize that these computations are made possible by the finiteness of our Hamiltonian matrix, Eq. (4), which allows us to obtain all the eigenstates with very high accuracy.

3.1. Individual Eigenfunctions

In this subsection we show some selected odd–odd eigenfunctions of the stadium action billiard. After diagonalizing the Hamiltonian matrix, we express the wavefunctions as

$$|\Psi^k\rangle = \sum_{n,m} C^k_{nm} |nm\rangle \tag{6}$$

where the indices n and m run in the set S defined in the previous section. Therefore, in the action representation, $|\Psi^k\rangle$ is given by a discrete set of numbers

$$\langle nm|\Psi^k\rangle = C^k_{nm} \tag{7}$$

Since θ plays the role of momentum in action billiards, plots of $|\langle nm|\Psi^k\rangle|^2 = |C^k_{nm}|^2$ are equivalent to plots of $|\Psi^k(x, y)|^2$ for common billiards. Therefore, we display contour plots of $|C^k_{nm}|^2$ for some relevant eigenstates of the stadium.

Figure 3 show the first six eigenstates, starting with the ground state at $E = -1.9819$. As in common billiards, the ground state exhibits a single maximum in the desymmetrized domain. The first excited state has one vertical nodal line, corresponding to one quantum of energy in the horizontal direction, while the second excited state has two, nearly vertical, nodal

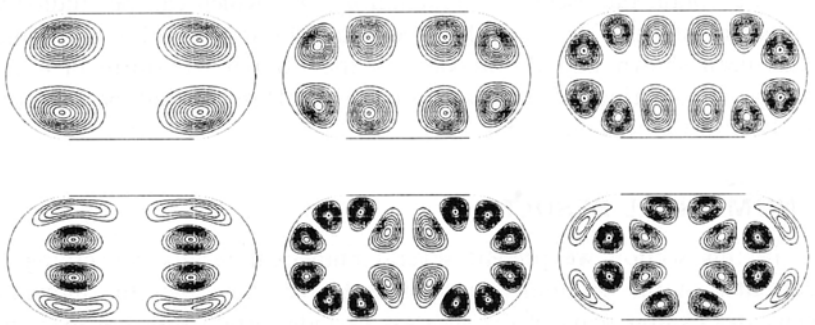

Fig. 3. First six odd–odd eigenstates of the stadium action billiard.

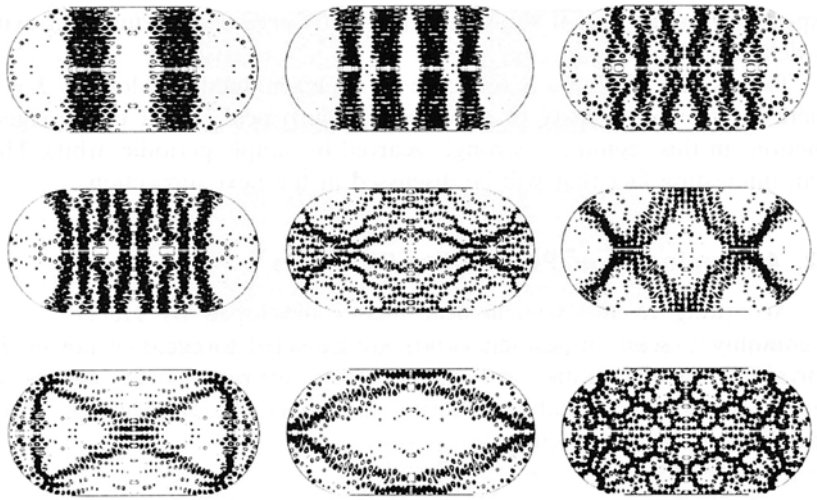

Fig. 4. Scars of periodic orbits in some excited eigenstates. (a–d) Scars of the vertical orbit at energies $E^{212} = -1.4621$, $E^{216} = -1.4544$, $E^{221} = -1.4444$, and $E^{229} = -1.4272$. (e–h) Scars of the horizontal, V-shaped, bowtie, and losangle orbits at $E^{341} = -1.1949$, $E^{316} = -1.2432$, $E^{280} = -1.3152$, and $E^{225} = -1.4343$, respectively. (i) An ergodic state at $E^{297} = -1.2834$.

lines. The third excited state has one horizontal nodal line and so forth. Therefore, the first excited states of the action billiard follow about the same structure as the corresponding states of the common stadium billiard.

Next, in Fig. 4 we show some selected highly excited eigenstates in the interval -1.5 to -0.5. As discussed in ref. 1, this is an interesting region, since the average density of states is nearly constant there and most of the periodic orbits satisfy $\partial\tau/\partial E \simeq 0$. Figures 4a–4d show scars of the vertical family with two, four, six and eight nodes, respectively. Figures 4e–4h show scars of the horizontal, the V-shaped, the bowtie, and the losangle orbits,

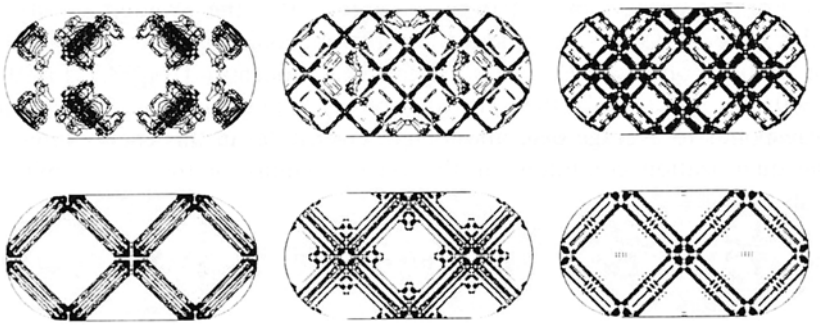

Fig. 5. Six consecutive eigenfunctions close to $E = 0$ with energies (a) -0.0020; (b) -0.0017, (c) -0.0013, (d) -0.0011, (e) 9.7×10^{-7}, and (f) 0.0000.

respectively, while Fig. 4i shows an apparently *ergodic* wavefunction, with no definite pattern.

Finally, Fig. 5 shows a sequence of six eigenfunctions close to $E=0$, where the average density of states has a sharp peak. Most of the eigenfunctions in this region are strongly scarred by simple periodic orbits. This is an interesting fact that will be discussed in the next subsection.

3.2. Averaging Over Probability Densities

According to the semiclassical theory developed by Heller[10] and Bogomolny,[5] scars of periodic orbits are expected to occur, if not in the individual eigenfunctions, at least in local averages over groups of wavefunctions after suitably smearing also over the coordinates. More explicitly, we define the quantity

$$P(E, \Delta E) = \left\langle \frac{1}{M} \sum_n |\Psi^n|^2 \right\rangle \tag{8}$$

where the sum runs in the interval ΔE centered at E, M is the number of wavefunctions within this interval, and the symbol $\langle \cdot \rangle$ means average over coordinates (remember that, even for action billiards, periodic orbits are parametrized by their energy). Then, for a given value of ΔE, scars of periodic orbits with periods $\tau \leqslant h/\Delta E$ will be observed at energies close to E if the quantization condition

$$\int p\, dq = (n + \alpha/4)\, h \tag{9}$$

is satisfied, where α is the Maslov index and the integration is along the orbit.

For the energy interval from -1.5 to -0.5, the average density of states is about 1.629×10^{-3}, and the shortest classical period is $\tau = 1.5$ for the vertical orbit at $E = -1.0$. Therefore, choosing $\Delta E = 13.325 \times 10^{-3}$ ($h = 0.020$) selects only the vertical orbit as a possible scar. This choice corresponds to average over about eight eigenstates in this energy interval. The quantization condition for the vertical family of the action billiard reads

$$\int \theta\, dI = nh \tag{10}$$

Figure 6 shows contour plots of $P(E, \Delta E)$ for $E = -1.3873$, -1.3856, -1.3839 and -1.3823. For the vertical orbit, the energy quantizes at

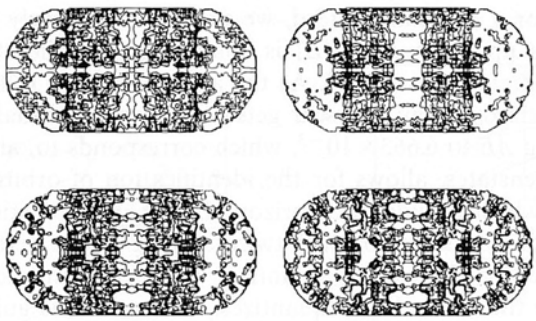

Fig. 6. Averaged probability density $p(E, \Delta E)$ over eight eigenstates for (a) $E = -1.3873$, (b) $E = -1.3856$, (c) $E = -1.3839$, and (d) $E = -1.3823$. The vertical orbit quantizes at $E = -1.3864$.

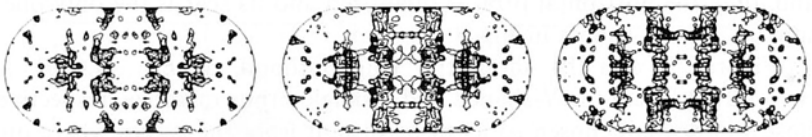

Fig. 7. Averaged probability density $P(E, \delta E)$ over four eigenstates for (a) $E = -1.3840$, (b) $E = -1.3822$, and (c) $E = -1.3804$. Both the vertical and the horizontal orbits quantize at $E = -1.3864$.

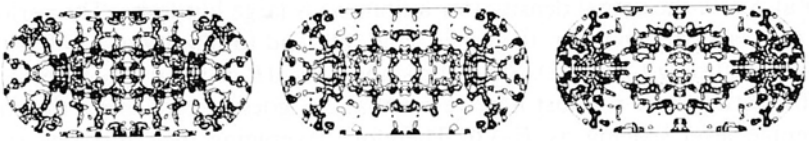

Fig. 8. Averaged probability density $P(E, \delta E)$ over four eigenstates for (a) $E = -1.3509$, (b) $E = -1.3491$, and (c) $E = -1.3466$. Here only the horizontal orbit quantizes at $E = -1.3510$.

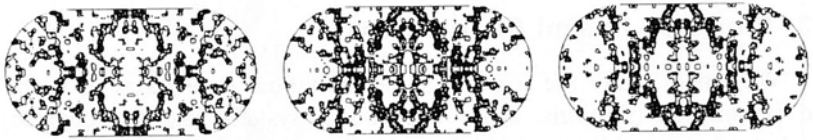

Fig. 9. Averaged probability density $P(E, \delta E)$ over four eigenstates for (a) $E = -1.0424$, (b) $E = -1.0401$, and (c) $E = -1.0386$. The V-shaped orbit quantizes at $E = -1.0490$.

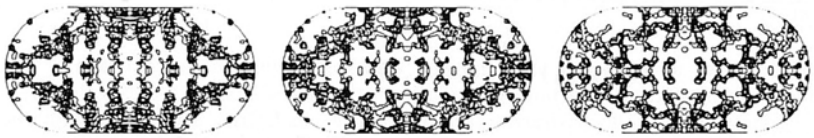

Fig. 10. Averaged probability density $P(E, \delta E)$ over four eigenstates for (a) $E = -1.2123$, (b) $E = -1.2103$, and (c) $E = -1.2085$. The losangle orbit quantizes at $E = -1.2252$.

$E = -1.3864$ for $n = 14$ and, indeed, we can see very clearly that the vertical scar shows up when $P(E, \Delta E)$ is computed with the states 244–251, whose averaged energy is 1.3857. As the average energy E is moved away from the quantized energy, the scar gets fainter and eventually disappears.

Decreasing ΔE to 6.663×10^{-3}, which corresponds to, an average over about four eigenstates, allows for the identification of orbits with periods up to $\tau \simeq 3.0$, which includes the horizontal, V-shaped, bowtie and losangle orbits. Since the horizontal orbit is twice as long as the vertical orbit, the energies where the horizontal quantizes will sometimes correspond to energies where the vertical also quantizes. In fact, this is going to happen at every other quantized horizontal energy. At $E = -1.3864$, for instance, both orbits are quantized and we should see their scars superimposed. This is indeed what happens, as shown in Fig. 7. At $E = -1.3822$, on the other hand, only the horizontal orbit is quantized and its scar is the only one to show up. This is shown in Fig. 8.

Figures 9 and 10 show the neighborhood of $E = -1.0401$ and $E = -1.2103$ where the V-shaped and losangle orbits quantize, respectively. Those values were chosen so as to be distant from the values where other orbits, such as the vertical and horizontal, quantize.

Now we go back to Fig. 5 and try to understand the scars close to $E = 0$. We notice that, although the average density of states, Eq. (5), blows up at $E = 0$, the actual density (for a finite $\hbar$) is large but finite. The periods of the classical orbits, on the other hand, all tend to infinity at $E = 0$, since $\mathbf{I} \to 0$ according to Eq. (2). Since the smoothing ΔE necessary to observe an orbit with period τ is just $\hbar/\tau$, we see that ΔE goes to zero faster than the average level spacing as $E \to 0$. Therefore, averaging over just one state (which means no averaging at all) is sufficient.

3.3. Projected Husimi Distributions

We finally study the scars of some individual eigenstates in terms of the Husimi distributions. Since our model system has two degrees of freedom, one possible way to look at the four-dimensional Husimi function is to project it down onto a canonical plane. Therefore, following ref. 11, we define

$$h_1(q_1, p_1) = \frac{1}{\pi} \int \langle z_1 z_2 | \Psi^k \rangle \, d^2 z_2$$

$$= \sum_{n, m, l} C^k_{m, l} C^k_{n, l} \frac{\bar{z}_1^n z_1^m \exp(-z_1 \bar{z}_1)}{(n!\, m!)^{1/2}}$$

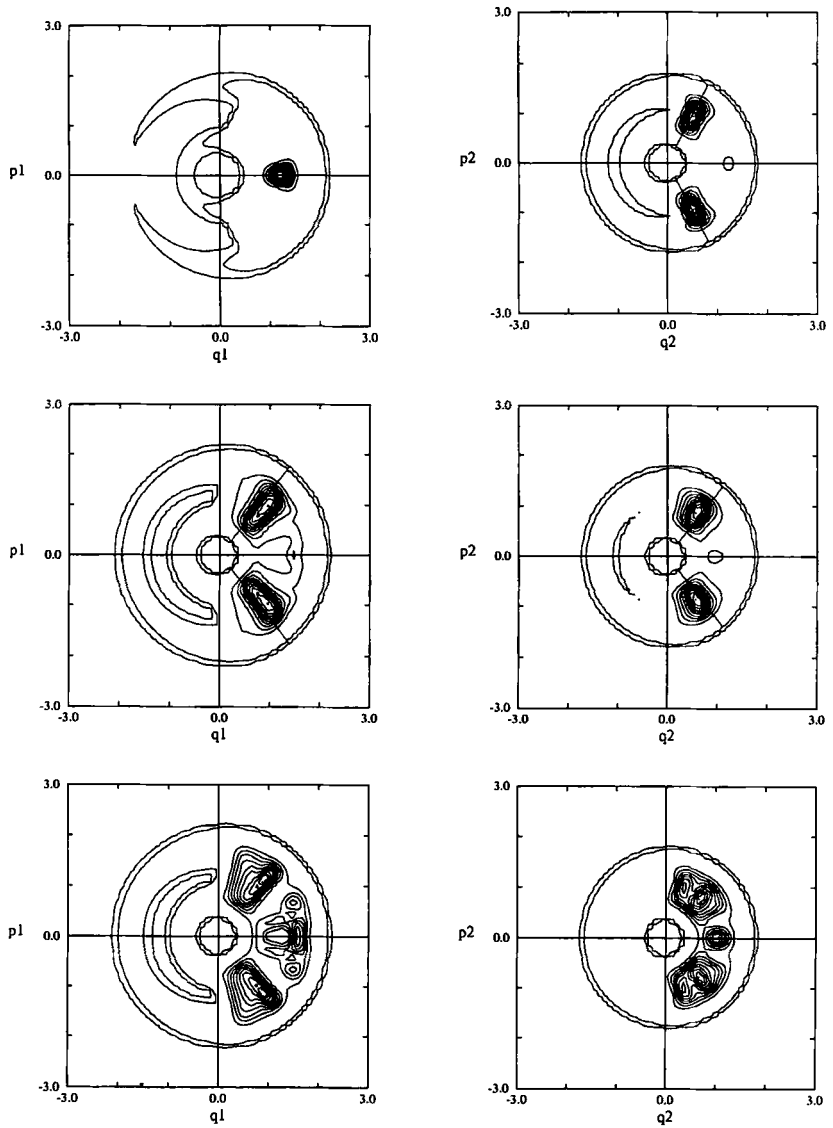

Fig. 11. Projections of the Husimi functions $h_1(q_1, p_1)$ and $h_2(q_2, p_2)$ for the eigenstates $E = -1.4621$, $E = 1.2432$, and $E = -1.2834$ (see Figs. 4a, 4f, and 4i). The thick lines in (a) and (b) are projections of the vertical and V-shaped orbits, respectively, at the same energy.

and

$$h_2(q_2, p_2) = \frac{1}{\pi} \int \langle z_1 z_2 | \Psi^k \rangle \, d^2 z_1$$

$$= \sum_{n,m,l} C^k_{m,l} C^k_{m,n} \frac{\bar{z}_2^l z_2^n \exp(-z_2 \bar{z}_2)}{(n!\, l!)^{1/2}}$$

where

$$|z_1 z_2\rangle = \exp\left(-\frac{z_1 \bar{z}_1}{2} - \frac{z_2 \bar{z}_2}{2}\right) \exp(z_1 a_1^\dagger + z_2 a_2^\dagger) \, |00\rangle \tag{11}$$

is the two-dimensional coherent state for the two-dimensional harmonic oscillator and

$$z_i = \frac{1}{\sqrt{2}} (q_i + i p_i)$$

In each of the two canonical planes, q_i versus p_i, the action billiard projects as a ring[1] bounded by the smallest and largest values of I_i. A vertical orbit with negative energy E, for instance, projects onto the (q_1, p_1) plane as $q_1 = \text{const}$, $p_1 = 0$ (or $\theta_1 = \pi$ and $I_1 = \text{const}$). On the (q_2, p_2) plane the same orbit projects as two radial lines at $\theta_2 = \pm \arccos(1 - E)$.

Figure 11 shows the projections $h_1(q_1, p_1)$ and $h_2(q_2, p_2)$ for the eigenstates 212, 316, and 297 (see Fig. 4), which correspond to scars of the vertical, horizontal, and a chaotic state, confirming that the scars also behave as in common billiards when observed in phase space.

4. CONCLUSIONS

The quantum mechanical billiard studied in this paper is completely different from the usual stadium billiard. Among the important differences is the fact that all eigenvalues lie in the range -2 to 2, since each $\cos \theta_i$ is itself limited to the range -1 to 1. In particular, this leads to a peculiar average (Weyl) density of states. Another important point is that the Hamiltonian cannot be separated into kinetic plus potential energies and both q and p change between two consecutive bounces at the boundary, while it is the angles that are kept constant. Nevertheless, the structure of the underlying classical periodic orbits is identical to that of the common stadium billiard. In ref. 1 we verified the validity of the GOE behavior of the spectral statistics and the contribution of individual periodic orbits to

its fluctuations. Here we have shown that the periodic orbits affect the eigenstates of the action billiard in much the same way as they affect the eigenstates of common billiards, providing again a dramatic confirmation of how these features are determined exclusively by the classical motion. Therefore, although the stadium action billiard is very much different globally from the common stadium billiard, in the limit $h \to 0$ the local properties, i.e., the quantum properties of a classically small energy interval, resemble the usual billiard in all respects.

These combined results show that action billiards are very interesting models for the study of quantum chaos and, in particular, to test the validity of the semiclassical propagator, since the quantum propagator can be computed exactly for all times.

One interesting remark on the practical side of computing eigenvalues is that boundary integral methods essentially reduce the 2D billiard to 1D, while the present billiards live in 2D explicitly. However, it should be noticed that a single matrix diagonalization provides *all* the eigenvalues of the action billiard, while boundary methods require continuous energy scans of a determinant to find the eigenenergies. Finally, we remark that, although strange at first sight, the Hamiltonian we have used in this work has a close relative in solid-state physics, where the divergence of the density of states at $E = 0$ is known as the Van Hove singularity.[12]

ACKNOWLEDGMENTS

It is a pleasure to thank Michel Baranger for fruitful suggestions. This paper was partly supported by CNPq, Fapesp, and Finep.

REFERENCES

1. A. M. Ozorio de Almeida and M. A. M. de Aguiar, *Chaos Solitons Fractals* **2**:377 (1992).
2. A. M. Ozorio de Almeida and M. A. M. de Aguiar, In *Quantum Chaos*, B. Chirikov and G. Casati, Eds. (Cambridge University Press, Cambridge, 1994).
3. M. A. M. de Aguiar and A. M. Ozorio de Almeida, *Nonlinearity* **5**:523 (1992).
4. M. A. M. de Aguiar, *Phys. Lett. A* **164**:284 (1992).
5. E. Bogomolny, *Physica D* **31**:169 (1988).
6. A. M. Ozorio de Almeida, In *Hamiltonian Systems: Chaos and Quantization* (Cambridge University Press, Cambridge, 1988).
7. D. Provost and M. Baranger, *Phys. Rev. Lett.* **71**:662 (1993).
8. A. M. Ozorio de Almeida, *Proc. R. Soc. Lond. A* **439**:139 (1992).
9. M. Baranger and M. A. M. de Aguiar, In preparation.
10. E. J. Heller, *Phys. Rev. Lett.* **53**:1515 (1984).
11. K. Furuya, M. A. M. de Aguiar, C. H. Lewenkopf, and M. C. Nemes, *Ann. Phys.* (N.Y.) **216**:313 (1992).
12. G. M. Zaslavsky *et al.* In *Weak Chaos and Quasi-Regular Patterns* (Cambridge University Press, Cambridge, 1991), Section 7.4.